



## DIFFERENT ROUTES FOR OBTAINING HYDROXYAPATITE BY SOL-GEL

Shirley J.M. Duarte<sup>1</sup>, Roseli M. Balestra<sup>2</sup>, Solange F. Nascimento<sup>3</sup>, Marize V. de Oliveira<sup>2</sup>, Magna M. Monteiro<sup>1</sup>

<sup>1</sup>Laboratorio de Bio y Materiales, Facultad Politécnica, Universidad Nacional de Asunción, San Lorenzo, Paraguay

<sup>2</sup>Laboratório de Tecnologia do Pó, Instituto Nacional de Tecnologia – INT, Rio de Janeiro (RJ), Brasil.

<sup>3</sup>Instituto Politécnico, Universidade Estadual de Rio de Janeiro, Nova Friburgo (RJ), Brasil.

E-mail: [sjoamduart@gmail.com](mailto:sjoamduart@gmail.com)

**Abstract.** Two routes for obtaining calcium phosphates by sol-gel technique are described. The ceramic precursors were calcium nitrate [ $\text{Ca}(\text{NO}_3)_2 \cdot 4\text{H}_2\text{O}$ ] and acid ammonium phosphate [ $(\text{NH}_4)_2\text{HPO}_4$ ]. The ammonium hydroxide (0.5 molar) was added in the solution in order to stabilize the pH to 9, approximately. The samples were analyzed by scanning electron microscopy with (SEM), X-ray diffraction (XRD) and Infrared spectrum (FTIR) to assess the morphology of the sintered powders, as well as present phases and crystallinity. In all samples it was observed the presence of crystals of hydroxyapatite accompanied by other phases, and one of the samples presented hydroxyapatite and  $\beta$ - Tricalcium phosphate phases, but it was not possible to identify the Hap/ $\beta$ -TCP weight ratios. It was found different morphologies of the particles depending on the route of synthesis and the particle size was submicrometric.

**Keywords:** Sol-gel, synthesis, Hap,  $\beta$ -TCP.

### 1. INTRODUCTION

Each year, there is a greater the number of people who have improved their quality of life and have even survival through biomaterials. The Hap  $\text{Ca}_{10}(\text{PO}_4)_6(\text{OH})_2$  is the main mineral component of bone (> 95%), therefore it has properties of biocompatibility and bioactivity that make it one of the most studied biomaterials to date, desirable for biomedical applications [Aoki, 1994, Ramakrishna et al., 2010, Rigo et al., 1999]. However, there are reports that sintered crystalline Hap ceramics have minimal resorption *in vivo*, thus delaying the formation of new bone [Metsger et al., 1982; Schmitz et al., 1999, Joschek et al., 2000; Kamakura et al., 2002, Hing et al., 2004]. For this reason, several studies have been performed based on the biocompatible biphasic calcium phosphate ceramic Hap- $\beta$ -TCP, due to the greater solubility of this phase, which disappears after the formation of new bone tissue [Tang et al., 2003, Kwon et al., 2003].

Several methods of Hap synthesis have been studied such as precipitation that involves reactions via wet medium in a solution containing  $\text{Ca}^{2+}$  and  $\text{PO}_4^{3-}$  with temperature and pH control [Bezzi et al., 2003, Santos et al., 2005]. The hydrothermal method, which has poor morphology control [Yoshimura et al., 1994]; the surfactant-assisted hydrothermal method is an improvement of the latter and it has been shown that the use of surfactant and further hydrothermal treatment favors to obtain nanorods with uniform morphology [Yan et al.,

2001]. Besides, Hap nanofibers have been obtained using suitable surfactant at ambient conditions [Liu et al., 2002] and Hap was prepared using a microemulsion route [Koumoulidis et al., 2003, Guo et al., 2005].

As reported by researchers, the sol-gel method presents certain advantages such as, homogeneous molecular mixing, low processing temperature and the ability to generate nanosized particles and nanocrystalline powders. In addition, this method is promising for the simplicity of the technological equipment used, low installation cost, the possibility of preparing films of low cost and the precise control of the films chemical composition [Rigo et al., 1999, Hwang et al., 2000, H-W Kim et al., 2004]. Thus, there are reports of several synthetic routes within the sol-gel method, studying different types of precursors, as well as the influence of temperature and aging time, agitation speed during the precursors mixing, different drying and calcination temperatures and the use of organic modifiers of particle size and phases found with such variants. All these researches present different Hap phase characteristics, according to the chemical composition and process conditions [Milev et al., 2003, Bezzi et al., 2003, Kim et al., 2004, Santos et al., 2005, Bogdanoviciene et al., 2006].

In this paper, different routes by sol-gel were studied, capable of achieving apatite phases for application as biomaterials. The study involved the development of a methodology which is able to prepare the phases in a large scale and with suitable reproducibility, without the need of several steps plus stringent precautions and careful manipulations to ensure the complete dissolution of precursors. A similar approach was proposed by Kim (2004) with cheap precursors, but with a considerably higher energy cost and processing time.

## **2. MATERIALS AND METHODS**

The reagents were as P.A., used without further purification. Each proposed method was named as I and II. For the method I, it was not considered the sequence of precursor's dissolution or that the rate of addition of the precursor solution on the other one can result in precipitation [Kim et al., 2004]. Instead, method II considered these factors. The prolonged step of refluxing (~ 24 h) was suppressed.

### **2.1 Materials**

Calcium nitrate tetrahydrate [ $\text{Ca}(\text{NO}_3)_2 \cdot 4\text{H}_2\text{O}$ ; Cicarelli, Title 99.0-103.0%], acid ammonium phosphate [ $(\text{NH}_4)_2\text{HPO}_4$ ; Cicarelli], ammonium hydroxide [ $\text{NH}_4(\text{OH})$ ; Biopack, Title 26%-30%] were used in these work.

### **2.2 Description of the different routes of preparation of the powder**

Method I: Calcium nitrate tetrahydrate and acid ammonium phosphate were dissolved in 210 mL of ammonia solution 0,569 N at room temperature, according to Bezzi (2003), but without the use of EDTA and urea, being the final solution  $\text{pH} > 9$ . The mixed solution was continuously stirred and maintained in the temperature range of 80 to 100°C for two hours. Then, heat treatment was performed with the sample in an oven from ambient temperature until 340°C, the heating rate being in the range of 4 – 5 °C/min until 250°C and then remaining at 250°C for one hour to continue with heating rate in the range of 4 – 5 °C/min until 340°C. The gum white paste obtained after drying was calcined at 800°C for two hours, being one hour the ramp time to reach 800°C. Finally the white powder obtained was stored for characterization without further treatment.

Method II: Stoichiometric amounts of calcium nitrate tetrahydrate and acid ammonium phosphate were dissolved in two separate aqueous solutions at room temperature. The pH was

adjusted to 9 in 0.5 N ammonia solution. The mixture was conducted by precursors dropwise, phosphate on nitrate, under constant agitation at room temperature. The white gel obtained was aged at a room temperature for four days. Then, the sample heat treatment was performed in an oven at 200 °C for one hundred minutes and then it was calcined at 800 °C for two hours, being one hour the ramp time to reach 800 °C.

### 2.3 Powder characterization

**X-ray diffraction (XRD).** To assess the present phases and crystallinity, the samples were analyzed by X-ray diffraction (X<sup>''</sup> Pert Pro-Panalytical Diffractometer) using a CuK $\alpha$  radiation generated at 40 kV and 40 mA, in the range of  $10^\circ < 2\theta < 90^\circ$  at a scan speed of 2 seg/pass, being 0,05° the pass size.

**Scanning electron microscopy (SEM).** The morphology of the synthesized Hap was studied and evaluated by scanning electron microscopy (SEM, FEI Inspect S) from CENANO/INT, operating at 20 kV on samples of Hap powder coated with gold through a metallizer EMITECH K550X operating at 25 mA for three minutes.

**Fourier transform infrared spectroscopy.** The infrared spectrum analysis by Fourier transform (FTIR) was performed by the "Magma - IR 560 Spectrometer ESP - Nicolet "to identify the functional groups in the sample. The FTIR spectra were recorded in the 500–4000 cm<sup>-1</sup> range, and compared with the spectra found in the literature. The sample was prepared with a proportion of 1% in KBr, i.e. 1mg of sample in 99mg of KBr.

## 3 RESULTS AND DISCUSSION

Figure 1, shows the XRD patterns of samples calcined at 800°C. In general, different phases were observed for each method. In the method II, a phase composed by Hap and  $\beta$ -TCP was observed.

For method I, the sample has the hydroxyapatite (Hap, ICDD N° 24-0033) phase and small peaks of calcium oxide (CaO) and calcium hydroxide (Ca(OH)<sub>2</sub>) phases. The CaO phase corresponds to the product of decomposition of the unreacted calcium nitrate. However, Ca(OH)<sub>2</sub> -decomposes in CaO at temperatures above 510°C. Thus, as the sample was calcined a 800°C, and theoretically the heat transfer is homogeneous within the muffle for all points of the system, the phase Ca(OH)<sub>2</sub> could be due to an insufficient time for the decomposition reaction was complete. The phases obtained are similar to those reported by Bezzi (2003), probably due to the similarity of both methods.

The XRD pattern for method II, identified Hap and  $\beta$ -tricalcium phosphate ( $\beta$ -TCP, ICDD N° 9-0169) phases. The corresponding diffraction peaks were very sharp, indicating the high crystallization of the two phases and suggesting that the crystal size obtained were relatively large. Is well known that this biphasic calcium orthophosphates, is used as biomaterials due to the higher biodegradability of  $\beta$ -TCP [S. Dorozhkin, 2012, A. Soueidan et al., 1995, M. Benahmed et al., 1996].

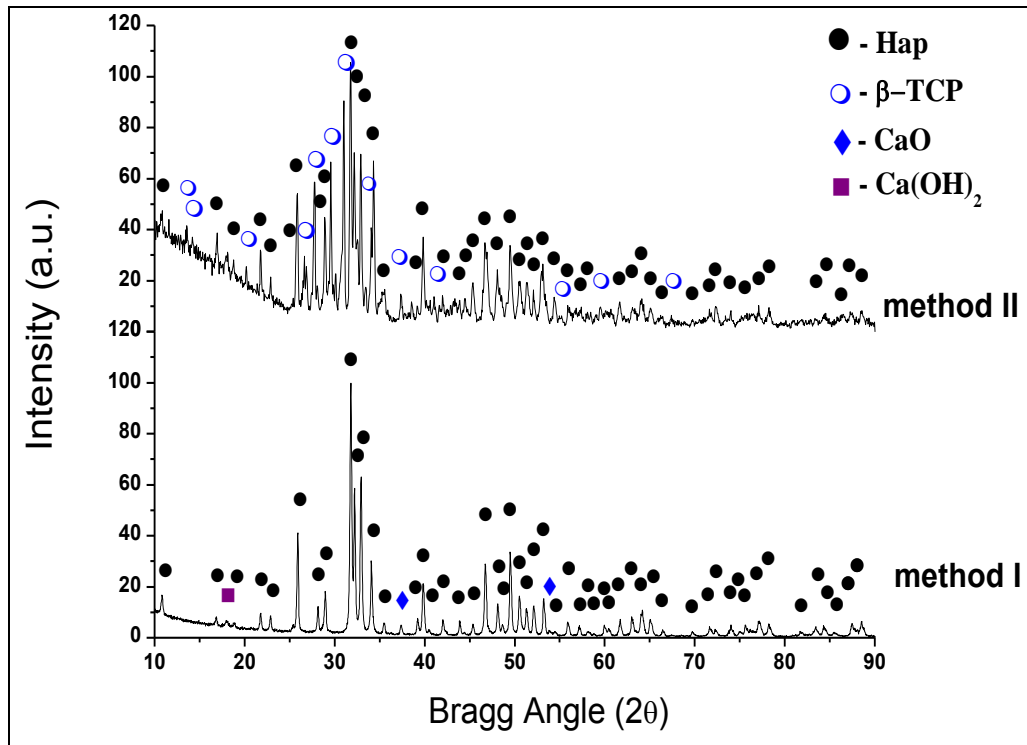


**Figure 1.** XRD diffractograms for the four methods tested.

Figure 2 presents FTIR patterns for as calcined calcium phosphates powders. The spectra for the method I and II are very similar.

The main absorption peaks of IR, can be attributed to the following functional groups [Santos et al., 1995, Posset et al., 1998, Arias et al., 1998, Mayor et al., 1998].

The phosphate group ( $\text{PO}_4^{3-}$ ), exhibit a strong, complex band in the  $1000\text{-}1065\text{ cm}^{-1}$  range corresponding to the asymmetrical stretching vibration with a shoulder at  $1085\text{ cm}^{-1}$ , and a medium intensity band at about  $960\text{ cm}^{-1}$  with a shoulder ( $945\text{ cm}^{-1}$ ) due to symmetric stretching vibration. The asymmetrical bending vibration is characterized by bands located at  $560\text{-}610\text{ cm}^{-1}$ .

The hydroxyl group ( $\text{OH}^-$ ), has a vibrational mode that appears at around  $634\text{ cm}^{-1}$  for the bending vibration and  $3570$  y  $3580\text{ cm}^{-1}$  for stretching vibration [Choi et al., 2004; Weng et al., 1998; Khelendra et al., 2011]. The  $\text{OH}^-$  stretching vibration is unique for crystalline hydroxyapatite and its intensity is considerably weaker compared to the strong P-O stretching vibration because of the hydroxyapatite stoichiometry [Nriagu et al., 1984]. The presence of an additional weak band at  $3645\text{ cm}^{-1}$  is attributed to the  $\text{OH}^-$  vibration from a  $\text{Ca}(\text{OH})_2$  phase [León et al., 2009]. However, others authors assign the sharp peaks  $3570$  of  $3670\text{ cm}^{-1}$  correspond to the stretching vibration of the lattice  $\text{OH}^-$  ions [Pramanik et al., 2005].

The broad absorption band of adsorbed water ( $\text{H}_2\text{O}$ ) can be observed in the range  $3700$  to  $2500\text{ cm}^{-1}$  and another peak at around  $1620\text{ cm}^{-1}$ . It would correspond to water stretching vibration, due to the hygroscopic character of the crystalline carbonated Hap [Koutsopoulos S., 2002; Suresh et al., 2012].

Additional peaks, appears in the  $1415\text{-}1462\text{ cm}^{-1}$  range, are associated with the asymmetrical stretching modes and weak band appearing at  $875\text{ cm}^{-1}$  related to the asymmetrical bending vibration. The positions of these peaks indicate the formation of B-type carbonated Hap [Koutsopoulos, 2002]. But the band of  $\text{CO}_3^{2-}$  group extends to  $1550\text{ cm}^{-1}$ , which could also indicate the presence of A-type carbonated Hap [Krajewski et al., 2005]. The carbonate ions substituted some phosphate ions in the apatite structure, for the Hap B-

type formed and replace the OH<sup>-</sup> ions in the A-type carbonated Hap [LeGeros et al., 1967, Bonel, 1972, Elliott, 1980]. The source of carbonate would have originated from CO<sub>2</sub> in the atmosphere [Wang et al., 2006].

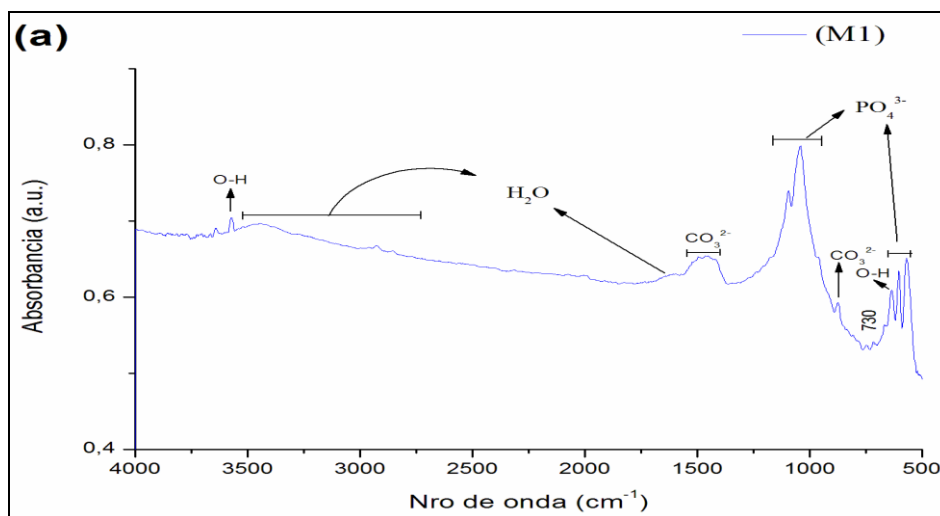
The type-B carbonated Hap is similar to natural bone mineral because bone mineral differs in composition from the stoichiometric Hap and carbonate ions are the most abundant additional ions. In vitro and in vivo test, have shown that the presence of B-type carbonate in the apatite structure, cause an increased in solubility of the same [Krajewski et al., 2005].

Physicochemical studies of Hap commercial applications as bone graft implant medical-dental, produced by four different manufacturers, have reported the presence of carbonate group in the samples [Conz et al., 2005].

Hap powders and biphasic calcium phosphate (BCP), containing phases Hap and  $\beta$ -TCP, obtained by sol-gel and calcined at temperatures  $\geq 600$  ° C, have been analyzed by FTIR, throwing the presence of carbonate in the same group [Salimi et al., 2012, Khelendra et al., 2011, Chen et al., 2011].

Results obtained by thermogravimetric analysis (TG), indicate temperatures of decomposition of the carbonate group for carbonated Hap, from 400 to 1200°C range [Krajewski et al., 2005]. Thus up to the maximum heat treatment temperature reached 800°C in this work, decomposition is not complete.

A small peak to 730 cm<sup>-1</sup> was observed in both methods. The same was not identified with literature data. However, it was mentioned that bands at 732.8 cm<sup>-1</sup> corresponding to the OH group, appear for samples of calcium phosphates containing phases of calcium pyrophosphate and TCP in the sample [Oliveira et al., 2009].



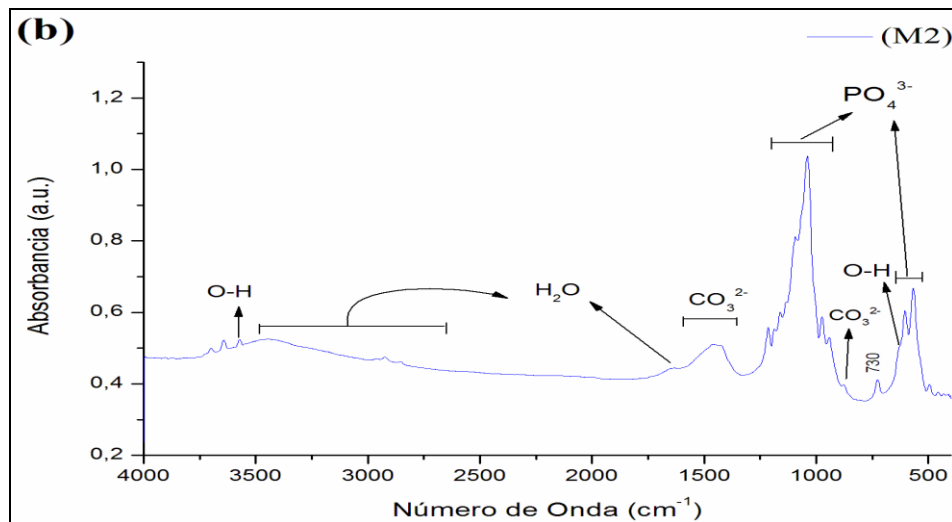


**Figure 2.** FTIR spectra of samples calcined at 800°C, (a) method I and (b) method II.

The SEM micrograph of the calcined powder for method I is displayed in two magnifications. In Fig. 3 (a) the powders exhibited the platelet like morphology of the sintered powders. In Fig. 3 (b) these particles appear spherical and highly agglomerated, as clusters of very small particles. Similar morphology was obtained by the sol gel method in other researches [Milev et al., 2003, Kim et al., 2004].

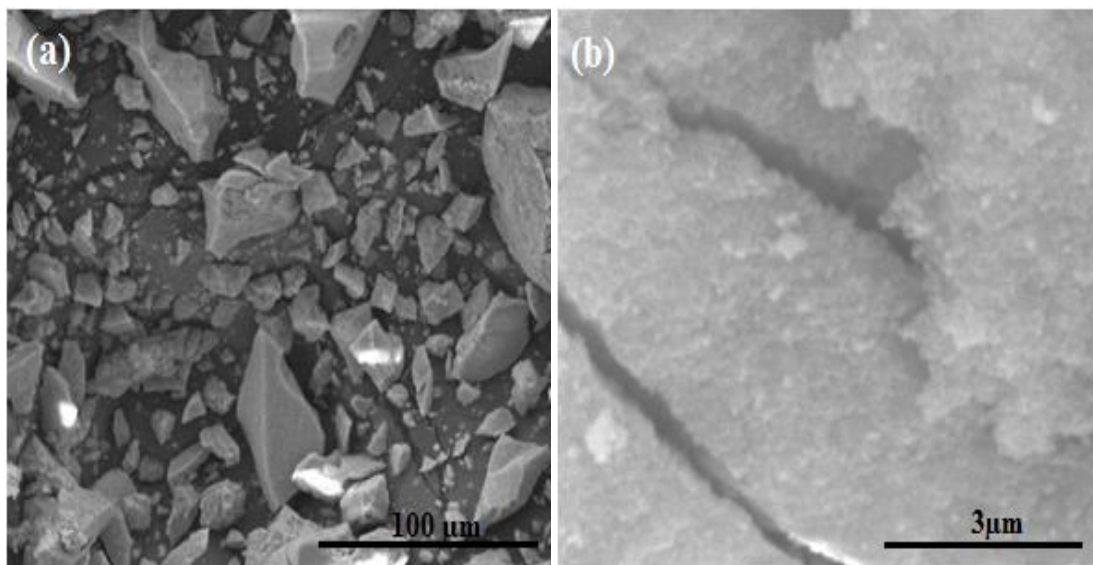


**Figure 3.** SEM micrograph of method I (a) 500X (b) 30000X.

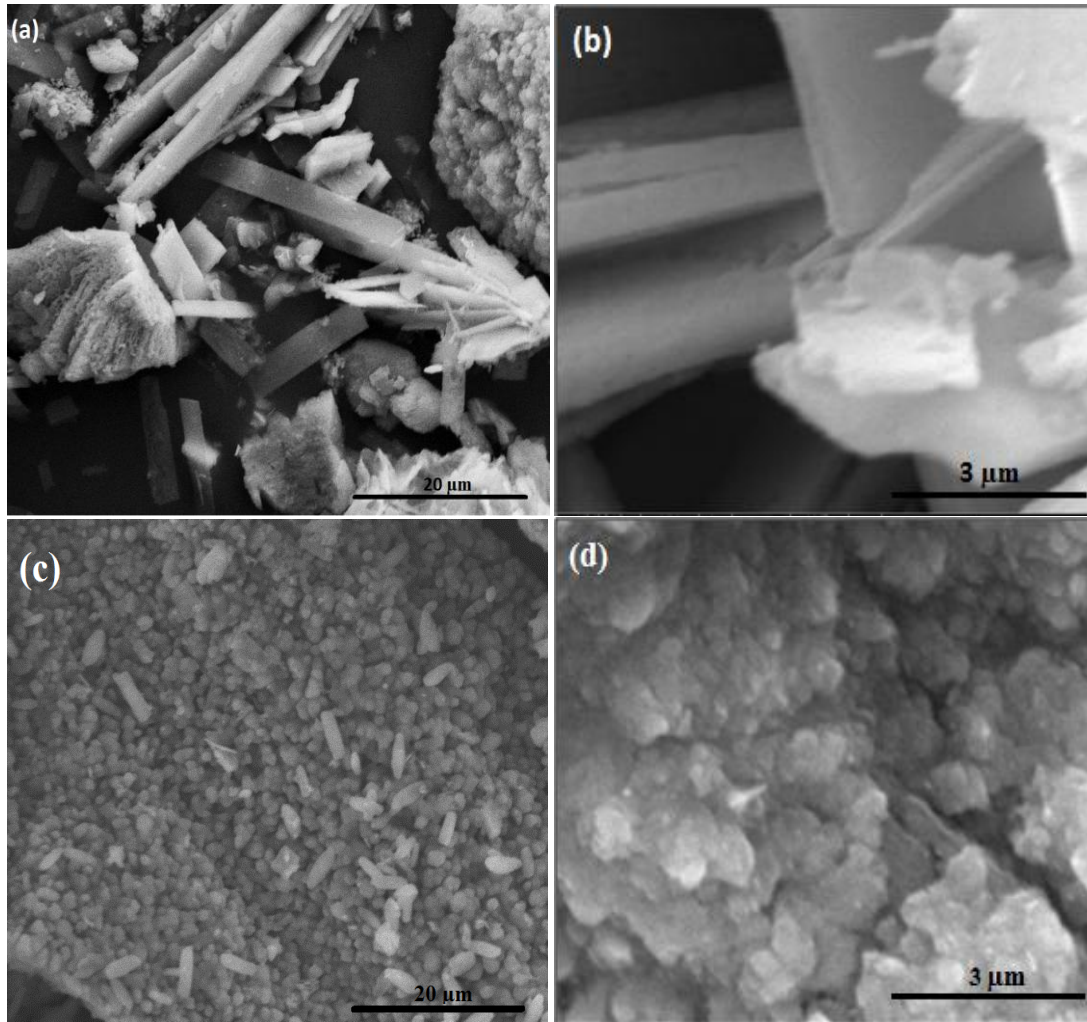
The Fig. 4, show the morphology of the calcined powder for method II. The particles exhibited two different morphologies. We analyze two cross sections of the found in two different increases. Already Santos (2005) has found clusters of various shapes and sizes from a Hap synthesized by sol-gel.

Figure 4 shows in (a) and (b), very fine elongated particles in the form of plates and rods (microrods), which are consistent with those obtained by sol-gel method in several articles [Yan et al., 2001, Bogdanoviciene et al., 2006, Murakami et al., 2012]. Other authors suggested the formation of whiskers for similar particle morphologies [Yoshimura et al., 1994, Roeder et al., 2006, Aizawa et al., 2005]. The whiskers are single crystals elongated,



generally has a cross-sectional diameter of 0.1-10 micrometers and lengths of 10-1000 micrometers. Synthesized apatite fibers appear to coincide with crystals that grow with preferred orientation to the axis c, parallel to the fibers longitudinal axis. But, in order to confirm this result we must perform TEM analysis of the individual fibers.

Nevertheless, Fig. 4 (c) and (d) show that platelets shaped particles were also obtained the same manner as in method I.



**Figure 4.** Method II SEM micrographs: particles in the form of rods, (a) 4000 X and (b) 30000 X; particles in the form of platelets, (c) 4000 X and (d) 30000X.

#### 4 CONCLUSIONS

The influence of the sol-gel synthesis route on the particle morphology and the phases obtained for calcium phosphate materials is evident. Moreover, it has been shown in this study that the sequence of the precursor's dissolution or that the different rates of solution addition of a precursor on the other, can give different results.

The techniques practiced in method I have developed the CaO and Ca(OH)<sub>2</sub> phases, which are not suitable for use as biomaterials, together with Hap phase. Those techniques practiced in the method II are very simple, inexpensive and produced calcium phosphate

particles, based in  $\beta$ -TCP and Hap, which are appropriate for use as biomaterial. However, these methods do not produced particles with uniform morphology, as occurred in method I.

In addition, FTIR indicated a calcium phosphate ceramics composed by carbonated hydroxyapatite in both methods. SEM images of the samples revealed the formation of particles with size micrometers, which is an important factor for the bone-implant attachment.

## ACKNOWLEDGEMENT

To “Concejo Nacional de Ciencia y Tecnología” (CONACYT) of Paraguay for the financial support.

Sheyla Carvalho of CENANO of Instituto Nacional de Tecnologia (INT), for the SEM micrographs.

Flavia de Almeida Ferreira of Laboratório de Catálise/LACAT of INT for to analized to FTIR.

## REFERENCES

- [1] M. Aizawa, A. E. Porter, S. M. Best, W. Bonfield. *Biomaterials* 26 (2005) 3427-3433.
- [2] Hideki Aoki. *Medical Applications of Hydroxyapatite* 94-75937; (1994).
- [3] J.L. Arias, F.J. García-Sanz, M.B. Mayor, S. Chiussi, J. Pou, B. León, M. Pérez-Amor. *Biomaterials* 19 (1998) 883.
- [4] Marcio Baltazar Conz, José Mauro Granjeiro, Gloria de Almeida Soares, Phisicochemical Characterization of Six Commercial Hydroxyapatites for Medical-Dental Applications as Bone Graft, *J Appl Oral Sci*, 2005, 13(2): 136-40.
- [5] M. Benahmed, J.M. Bouler, D. Heymann, O. Gan, G. Daculsi. *Biomaterials* 17 (1996) 2173-2178.
- [6] G. Bezzi, G. Celotti, E. Landi, T.M.G. La Torretta, I. Sopyan, A. Tampieri. *Mat Chem Phys* 78 (2003) 816-824.
- [7] I. Bogdanoviciene, A. Beganskiene, K. Tõnsuaadu, J. Glaser, H.-J. Meyer, A. Kareiva. *Mat Res Bull* 41 (2006) 1754-1762.
- [8] G. Bonel, *Ann. Chim.* 7 (1972) 65.
- [9] Jingdi Chen, Yingjun Wang, Xiaofeng Chen, Li Ren, Chen Lai, Wen He, Qiqing Zhang. A simple sol-gel technique for synthesis of nanostructured hydroxyapatite, tricalcium phosphate and biphasic powders. *Mater Lett* 65 (2011) 1923-1926.
- [10] D. Choi, K. Marra, P.N. Kumta, 2004, “Chemical synthesis of hydroxyapatite/poly ( $\epsilon$ -caprolactone) composite”, *Materials Research Bulletin*, Vol.39, pp. 417-432.
- [11] S.V. Dorozhkin, *Acta Biomaterialia* 8 (2012) 963-977.
- [12] J.C. Elliott, *J. Appl. Cryst.* 13 (1980) 618.
- [13] G. Guo, Y. Sun, Z. Wang, H. Guo. *Ceram Int* 31 (2005) 869-872.
- [14] K.A. Hing, S.M. Best, K.E. Tanner, W. Bonfield, P.A. Revell. *J Biomed Mater Res* 68 (2004) 187-200.
- [15] K. Hwang, J. Song, B. Kang, Y. Park. *Surf Coat Tec* 123 (2000) 252-255.
- [16] S. Joschek, B. Nies, R. Krotz, A. Goepferich. *Biomaterials* 21 (2000) 1645-1658.
- [17] S. Kamakura, Y. Sasano, T. Shimizu, K. Hatori, O. Suzuki, M. Kagayama, K. Motegi. *J Biomed Mater Res* 59 (2002) 29-34.
- [18] Khelendra Agrawal, Gurbhinder Singh, Devendra Puri, Satya Prakash, *Journal of Minerals & Materials Characterization & Engineering*, Vol. 10, No.8, pp.727-734,2011.
- [19] I. Kim, P.N. Kumta. *Mat Sci Eng B*111 (2004) 232-236.
- [20] H-W. Kim, H-E. Kim, V. Salih, J.C. Knowles. *Wiley Interscience* (2004) DOI: 10.1002/jbm.b.30073.
- [21] G.C. Koumoulidis, A.P. Katsoulidis, A.K. Ladavos, P.J. Pomonis, Ch. C. Trapalis, A.T. Sdoukos, T.C. Vaimakis. *J Coll Inter Sci* 259 (2003) 254-260.
- [22] Koutsopoulos S. Syntjesis and characterization of hydroxyapatite crystals: a review study on the analytical methods. *J Biomed Mater Res* 2002;62:600-12.
- [23] Krajewski A., M. Mazzocchi, P.L. Buldini, A. Ravaglioli, A. Tinti, P. Taddei, C. Fagnano. Synthesis of carbonated hydroxyapatites: efficiency of the substitution and critical evaluation of analytical methods, *Journal of Molecular Structure* 744-747 (2005) 221-228
- [24] S.H. Kwon, Y.K. Jun, S.H. Hong, H.E. Kim. *J Eur Ceram Soc* 23 (2003) 1039-1045.
- [25] R.Z. LeGeros, O.R. Trauz, J.P. LeGeros, *Science* 155 (1967) 1409.



- [26] B. León, J.A. Jansen. In: *Thin Calcium Phosphate Coatings for Medical Implants*. (Springer Science + Business Media, LLC (2009), p. 26.
- [27] Y. Liu, W. Wang, Y. Zhan, Ch. Zheng, G. Wang. *Mat Lett* 56 (2002) 496-501.
- [28] B. Mayor, J. Arias, S. Chiussi, F. García, J. Pou, B. León and M. Pérez-Amor, *Thin Solid Films* 317 (1998) 363.
- [29] D.S. Metsger, T.D. Driskell, J.R. Paulsrud. *J Am Dent Assoc* 105 (1982) 1035-1038.
- [30] A. Milev, G.S.K. Kannangara, B. Ben-Nissan. *Mat Lett* 57 (2003) 1960-1965.
- [31] S. Murakami, K. Kato, Y. Enari, M. Kamitakahara, N. Watanabe, K. Ioku. *Cer Int* 38 (2012) 1649-1654.
- [32] M. Nabil Salimi, Rachel H. Bridson, Liam M. Grover, Gary A. Leeke. *Powder Technology* 218 (2012) 109-118.
- [33] J.O. Nriagu, B.P. Moore (Eds.), *Phosphate Minerals* Springer, Berlin, 1984.
- [34] S.V. Oliveira, K.M. Medeiros, E.P. Araújo, C.R.C. Braga, E.M. Araújo, M.V.L. Fook. *Revista Electrónica de Materiales y Procesos*, v.4.3 (2009) 11-20.
- [35] Posset, E. Löcklin, R. Thull, W. Kiefer. *J. Biomed. Mater. Res.* 40 (1998) 640.
- [36] Pramanik Sumit, Avinash Kumar Agarwal, K.N. Rai. *Development of High strength Hydroxyapatite for Hard Tissue Replacement*, *Trends Biomater. Artif. Organs*, Vol 19 (1), pp 46-51 (2005).
- [37] S. Ramakrishna, M. Ramalingam, T.S.S. Kumar, W.O. Soboyejo. *Biomaterials A Nano Approach* 978-1-4200-4781-3; (2010).
- [38] R. K. Roeder, G. L. Converse, H. Leng, W. Yue. *J Am Ceram Soc* 89[7] (2006) 2096 – 2104.
- [39] E.C.S. Rigo, L.C. Oliveira, L.A. Santos, A.O. Bosch, R.G. Carrodeguas; *Hydroxyapatite coatings on metals*; *Revista Brasileira de Engenharia Biomédica* v. 15, n. 1-2, p. 21-29; (1999).
- [40] M.L. Santos, A.O. Florentino, M.J. Saeki, A.H. Aparecida, M.V. Lia Fook, A.C. Guastaldi. *Ecl Quim* 30(3) (2005) 29-35.
- [41] R.V. Santos, R.N. Clayton, *American Mineralogist* 80 (1995) 336.
- [42] J.P. Schmitz, J.O. Hollinger, S.B. Milam. *J Oral Maxillofac Surg* 57 (1999) 1122-1126.
- [43] A. Soueidan, O.I. Gan, J.M. Bouler, F. Goin, G. Daculsi. *Cells Mater* 5 (1995) 31-44.
- [44] G. Suresh Kumar, A. Thamizhavel, E.K. Girija. *Microwave conversion of eggshells into flower-like hydroxyapatite nanostructure for biomedical applications*. *Materials Letters* 76 (2012) 198-200.
- [45] R. Tang, M. Hass, W. Wu, S. Gulde, G.H. Nancollas. *J Colloid Interface Sci* 260 (2003) 379-384.
- [46] Wang YJ, Chen JD, Wei K, Zhang SH, Wang XD. *Surfactant-assisted synthesis of hydroxyapatite particles*. *Mater Lett* 2006;60:3227-31.
- [47] W. Weng, J.L. Baptista, 1998, “Sol-gel derived porous hydroxyapatite coatings”, *Journal of materials science: materials in medicine*”, Vol. 9, pp. 159-163.
- [48] L. Yan, Y. Li, Z. Deng, J Zhuang, X. Sun. *J Inorg Mater* 3 (2001) 633-637.
- [49] M. Yoshimura, H. Suda, K. Okamoto, K. Ioku. *J Mat Sci* 29 (1994) 3299-402.